Journal of Computers Vol. 32 No. 3, 2021, pp. 222-236
doi:10.3966/199115992021063203016

The Dynamic Characteristics of Marching Fire of Armored Vehicle Based on ADAMS Launch Dynamics and Virtual Reality

Chao Song, Hong-Tian Liu*, Dong-Jun Wang, Bing Ji, Yi-Zhuo Jia

Department of Weapons and Control, Army Academy of Armored Forces, Beijing, China
andysong475@163.com, zgyliuhongtian@sohu.com, wdogw@sina.com, jibing7506@sohu.com, tyututy@126.com

Received 17 April 2021; Revised 1 May 2021; Accepted 17 May 2021

Abstract. In order to improve the combat efficiency of armored vehicles, the dynamic performance of marching fire of armored vehicles is studied. Firstly, hypothesis analysis is made on the force characteristics of marching fire of armored vehicle. Secondly, the dynamics model of marching fire of the wheeled armored vehicle is built by using ADAMS dynamics software, and the marching fire of armored vehicle is simulated by using virtual reality (VR). Finally, the accuracy of the dynamic analysis model is analyzed, and the firing conditions under different situations are analyzed empirically. The results of the study show that the error range between the dynamic analysis model of marching fire of the armored vehicle and the actual test value is within 15%, indicating that the analysis method proposed has a certain accuracy. The worse flatness level of the driving road surface is, the worse firing stability of the armored vehicle is. The increase of high and low angles of fire leads to the increase of muzzle disturbance amplitude. The increase of the directional firing angle and the trunnion clearance will lead to the gradual change of the displacement of high and low angles and the displacement of direction angles of the muzzle. Through research, the proposed analysis method has a certain accuracy. It is hoped that it can provide a certain reference basis for the optimization of the combat parameters of marching fire of armored vehicle, and improve the combat efficiency of the armored vehicle.

Keywords: ADAMS, VR, marching fire, dynamic analysis

1 Introduction

In recent years, with the continuous development of combat weapons, many weapons have been loaded on armored chassis. New vehicle-mounted weapons such as self-propelled artillery and anti-aircraft missile launch vehicles have appeared one after another. Combat methods have also been changed. Due to its characteristics, vehicle-mounted weapons need to undertake multiple tasks such as the fast maneuver, ground penetration, suppression, and air defense in wars. The implementation of marching fire with vehicle-mounted weapons is the primary condition for ensuring full operational efficiency and improving their battlefield survivability. With the continuous updating of modern warfare modes, traditional static combat methods can no longer meet the requirements of current combat. Therefore, some vehicle-mounted weapons now have the ability of marching fire. Many investigations have proved that muzzle disturbance is the main factor affecting shooting accuracy. During the driving of the vehicle-mounted weapon, the flatness of the road surface and the change of the vehicle speed will affect the muzzle vibration, further influencing the shooting accuracy of the vehicle-mounted weapon. At the same time, due to the characteristics of the vehicle-mounted weapon, its barrel will be elastically deformed during the driving state. The barrel will contact and collide with the lining tile. Also, there will be a clearance between the trunnion and the assembly of the trunnion chamber. These factors will cause a

* Corresponding Author

complex vibration state of the muzzle. Currently, there is no method to explore the marching fire dynamics of vehicle-mounted weapons while taking all factors into consideration.

Therefore, the dynamic characteristics of the marching fire of armored vehicles are taken as the research topic. With the aid of the dynamic analysis software ADAMS and virtual reality technology, the dynamic characteristics of marching fire of the wheeled self-propelled AA gun are modeled and analyzed. The dynamic characteristics of the muzzle of armored vehicles under different road conditions, different firing conditions, and different trunnion clearances are explored. It aims to provide a certain theoretical foundation and engineering application value for improving the firing accuracy and combat performance of vehicle-mounted weapons.

2 Background and Related Work

The armored vehicle is a multi-body dynamics system. In the last century, some scholars used the graph theory method and Kane method to study multi-body dynamics, which laid a theoretical foundation for the study of multi-body dynamics [1]. With the continuous deepening of the research on the dynamic characteristics of marching fire of the vehicle-mounted armored vehicles, the launch dynamics model is constantly advancing in the direction of large-scale, complex, and nonlinear. The current multi-body dynamics analysis software such as ADAMS can greatly improve the efficiency of armored vehicle dynamics modeling and ensure the accuracy of calculation results. At present, Chinese research on marching fire technology is mainly carried out from two aspects: the impact of the armored vehicle chassis on the launch power, as well as the impact of the vehicle accessories on the barrel and the dynamic response on the marching [2]. Although considerable progress has been made, most of the current roughness models established for armored vehicle marching are two-dimensional models. They cannot analyze the impact of changes in road roughness caused by tire width and vehicle yaw. Also, the current calculation of marching fire dynamics is mainly to analyze and explore the impact of different levels of the road surface, vehicle speed, and other parameters on the muzzle [3]. However, changes in multiple structural parameters such as different heights, directional firing angles, trunnions, bearings, and barrels will cause changes in the muzzle response. The impact of these factors on the marching fire dynamics still needs further study.

Therefore, the force status of the armored vehicle on the marching is first analyzed for the deficiencies in the current research. Then, when analyzing the armored vehicle system, it is simplified to a multi-rigid-body system, while making an idealized assumption. Second, the ADAMS dynamics software is used to build the dynamic model of the marching fire of wheeled armored vehicles. At the same time, the virtual reality (VR) is used to carry out the simulation training for the marching fire of armored vehicles. Finally, the dynamic characteristics of the armored vehicle on the marching are analyzed from the marching comfort, different heights, directional firing angles, and trunnion clearance.

3 Methods

3.1 Armored Vehicle

Armored vehicles have the maneuvering performance of general vehicle systems. In addition, it also has a weapon system that combines firepower attack and armor protection functions [4]. The driving mechanism of armored vehicles is determined according to different combat environments and combat missions. Generally speaking, armored vehicles also have higher off-road performance and higher driving speed. In order to ensure the survival efficiency of personnel in a complex battlefield environment, the body and turret of the armored vehicle are covered with armor, so that the armored vehicle has strong protection capabilities. The armored vehicle system can be divided into two parts: artillery and chassis [5].

The chassis system of armored vehicles can be divided into two types: wheeled chassis and tracked chassis due to different driving mechanisms. These two types include the body of the armored vehicle, body components, power system, transmission system, steering system and braking system. The artillery system is composed of the rear seat part, the landing part and the rotary part of the armored vehicle.

3.2 Force Analysis of Marching Fire of Armored Vehicles

Armored vehicle is a complex system composed of multiple components. Complex displacement, elastic deformation and load transfer will occur in marching fire of the mechanical system [6]. From a physical point of view, armored vehicle is a typical system of multi-body dynamic. The analysis of the marching fire characteristics of armored vehicles is complicated. In order to facilitate the analysis of the force of marching fire system of the armored vehicle, it is necessary to simplify the force and motion status of the components of the armored vehicle during matching. Therefore, in the analysis, it needs to be simplified and idealized: First, all the components of the armored vehicle are regarded as rigid bodies, so there is no need to consider the elastic deformation of the components and the nonlinear effects occurring between the components; Second, it is considered that the constrained connection between all parts of the system is ideal, and the coupling effect between projectile and barrel is not considered when firing. It is considered that the contact between crawler plate and pavement of crawler chassis is rigid contact, while the elastic deformation of wheeled chassis is only calculated. Finally, the stabilizing effect of the body tube of the fire control system is not taken into account when the armored vehicle is marching, and the loads of the balancing machine, repositioning machine and reentry machine of the armored vehicle are defined by the functions of generalized coordinates, generalized speed and mechanism size [7].

3.2.1 The Dynamics of Chassis System of Marching Fire of Armored Vehicles

The dynamics of the chassis system of marching fire of armored vehicles is analysed. Tank is one kind of armored vehicles, which is the most complicated system structure in the armored vehicle. Therefore, the dynamic model of other types of armored vehicles can be obtained by simplifying the model construction of tank dynamics [8]. The tank system is generally composed of a car body, as well as $2n$ loading wheels and tracks distributed on both sides. When the tank is in motion, the movement variable of the tank vehicle system is:

$$S_0 = (\xi, \zeta, \gamma)^T, \tag{1}$$

$$v_0 = (\xi', \zeta', \gamma)^T. \tag{2}$$

Where: S_0 and v_0 refer to the displacement and speed vector of the vehicle respectively. ζ is the linear velocity of the vehicle marching horizontally along the x-axis. ξ is the linear displacement of the vehicle marching horizontally along the x-axis. ξ' and ζ' are the linear displacement and linear velocity of the vehicle moving laterally along the y-axis. γ and γ' are the displacement of heading angular and angular velocity of the vehicle rotating around the z-axis.

The calculation method of motion variables of the tank body is shown below.

$$S_1 = (\eta, \theta, \phi')^T, \tag{3}$$

$$v_1 = (\eta', \theta', \phi')^T. \tag{4}$$

Where: S_1 and v_1 represent the displacement and speed vector of the vehicle body. η' is the linear velocity of the vehicle body marching horizontally in the direction of the z-axis. η is the linear displacement of the vehicle body marching horizontally in the direction of the z-axis. θ and θ' are the displacement of pitch angular and angular velocity of the vehicle's lateral movement along the y-axis. φ and φ' refer to the displacement of roll angular and angular velocity of the vehicle body rotating around the x-axis.

The calculation method of the motion variable of the loading wheel is as follows.

$$S_2 = (S_{2L}, S_{2R})^T, \tag{5}$$

$$v_2 = (v_{2L}, v_{2R})^T. \tag{6}$$

Where: S_{2L} and S_{2R} represent the displacement vector of the left and right loading wheels, respectively. v_{2L} and v_{2R} represent the speed vector of the left and right loading wheels, respectively.

Therefore, the calculation of the main power F_0 and the resistance vector R_0 of the entire tank is as follows.

$$F_0 = (F_x, F_y, M_0)^T, \tag{7}$$

$$R_0 = (R_x, R_y, L_0)^T. \tag{8}$$

Where: F_x and F_y are the main power acting on the vehicle along the x-axis direction and y-axis direction. R_x and R_y are the resistance acting on the vehicle along the x-axis direction and y-axis direction. M_0 is the main power moment acting on the vehicle while rotating around the z-axis, and L_0 is the resistance moment acting on the vehicle while rotating around the z-axis.

The calculation method of the generalized interference vector F_1 acting on the vehicle body is as follows.

$$F_1 = (P_c, M_x, M_y)^T. \tag{9}$$

Where: P_c is the vertical interference force in the z-axis direction received by the vehicle body. M_x and M_y are the interference torques received by the vehicle body in rotation around the x-axis and y-axis.

The calculation method of the elastic restoring force vector F_{K1} and the damping force vector F_{C1} of the suspension device is as follows.

$$F_{K1} = (F_{K1L}, F_{K1R})^T, \tag{10}$$

$$F_{K1} = (F_{K1L}, F_{K1R})^T. \tag{11}$$

Where: F_{K1L} and F_{K1R} represent the elastic restoring force of the left and right suspension devices of armored vehicles. F_{C1L} and F_{C1R} represent the damping force of the left and right suspension devices of armored vehicles.

The calculation of the elastic recovery force F_{K2} and F_{K3} of the track acting between the loading wheel and the ground is shown below.

$$F_{K2} = (F_{K2L}, F_{K2R})^T, \tag{12}$$

$$F_{K31} = (F_{K3L}, F_{K3R})^T. \tag{13}$$

Where: F_{K2L} and F_{K2R} represent the loading wheels on the left and right sides of the armored vehicle. F_{K3L} and F_{K3R} represent the elastic recovery force of the track on the left and right sides of the armored vehicle.

The expression method of the track elastic restoring force vector F_N acting between the loading wheel and the ground is as follows.

$$F_N = (0, 0, 0, F_{\phi_y})^T. \tag{14}$$

Where: $F_{\varphi Y}$ is the restraint damping moment of the roll structure of the vehicle body.

3.2.2 Dynamics of Firepower System of Marching Fire of Armored Vehicles

The firepower part of the armored vehicle is analyzed, and the turret quality of the armored vehicle is assumed to be M_t. The disturbance moment M_d of vehicle body received by the turret during moving fire is calculated by as follows.

$$M_d = M_t \cdot g \cdot e_t(\sin\theta \cdot \sin\psi_t + \sin\phi \cdot \cos\psi_t + \gamma + a_x \sin\psi_t + a_y \cos\psi_t). \tag{15}$$

Where: θ is the pitch angle displacement, and φ is the roll angle displacement; γ refers to the acceleration of the yaw angle, a_x refers to the acceleration of the vehicle along the x-axis of the driving direction, and a_y is the acceleration of the vehicle along the y-axis; Ψ_t is the angular velocity of the turret rotation, and g is the acceleration of gravity.

During the rotation of the turret, the friction torque $M_f$received is:

$$M_f = f_t \cdot M_t \cdot g \cdot R_t(\cos\theta + \sin\theta). \tag{16}$$

Where: R_t is the turning radius of the turning part, and f_t is the friction coefficient of the race ball and the inner and outer raceways.

When firing, the torque M_r received by the turret is:

$$M_r = R(t) \cdot e_r \cdot \tag{17}$$

Where: $R(t)$ refers to the recoil resistance of the turret, and e_r is the eccentricity of the barrel axis relative to the center of rotation.

The rotational inertia of the turret rotation is set to J_t, the angular displacement of the turret rotation is regarded as Ψ_t, and the kinetic equation $J_t\psi$ of the turret's rotation movement can be obtained as shown below.

$$J_t\psi = M_d - M_f - M_r \cdot \tag{18}$$

The expression of the equation of center of mass dynamic of the vehicle during driving is shown below.

$$\delta \frac{G}{g} \frac{dv}{dt} = R_e - R_t \cdot \tag{19}$$

Where: v refers to the driving speed of the vehicle, t is the driving time of the vehicle, and G is the total weight of the vehicle system. δ refers to the increase coefficient of the vehicle quality, R_e refers to the measured driving power, and R_t refers to the driving resistance of the vehicle.

When the tank movies in a straight line, the vehicle and all its components are moving in an associated translational motion. Some components of the power unit, transmission, and formal device are in relative motion. The motion of a tracked vehicle includes both relative motion and relative rotary motion, while wheeled vehicles only perform relative rotary motion. Therefore, the calculation method of the total kinetic energy of the vehicle running can be obtained as shown below.

$$E = E_q + E_x \cdot \tag{20}$$

Where: E_q refers to the kinetic energy of the vehicle in the implicated translational motion, and E_x is the kinetic energy of the relative motion and rotary motion of the component.

3.3 Dynamic Analysis of Marching Fire of Armored Vehicles

The dynamic analysis of marching fire of armored vehicle is more complicated than shooting at rest. For the dynamic analysis of marching fire of armored vehicle, it is necessary to consider not only the dynamic characteristics of the artillery part of the armored vehicle, but also the impact of the road surface factors of the armored vehicle in the actual combat environment on the vibration of the armored vehicle chassis. Therefore, in order to ensure the accuracy and precision of the analysis when analyzing the dynamic characteristics of marching fire of the armored vehicle, the chassis system of the armored vehicle needs to be accurately analyzed. The workflow for analyzing the dynamic characteristics of marching fire of armored vehicles is shown in Fig. 1 below.

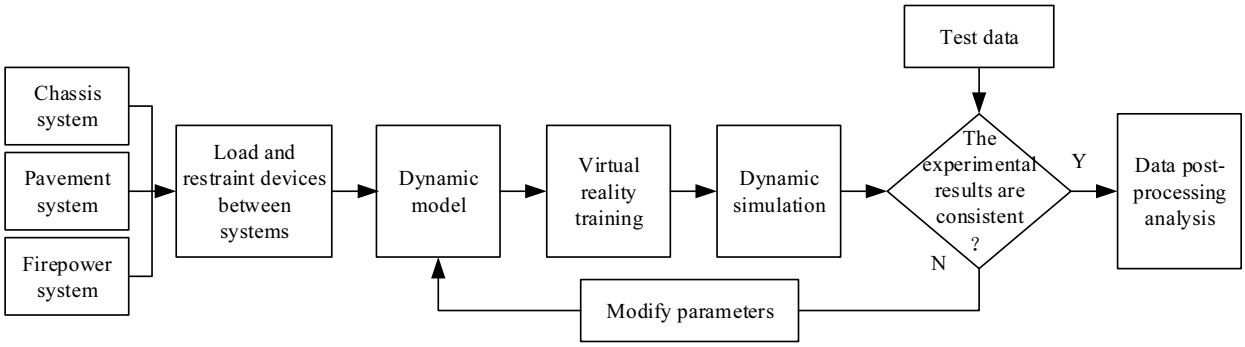

Fig. 1. Flow chart of the analysis of the dynamic characteristics of marching fire of armored vehicles

3.3.1 ADAMS Software

ADAMS software is a dynamic analysis method that uses the first type of Lagrangian method in the dynamic theory of multi-rigid-body systems to establish the dynamic equations of mechanical systems [9]. It uses Cartesian coordinates of the center of mass of the rigid body and Euler angles representing the orientation of the rigid body to establish generalized coordinates. When using ADAMS software to solve dynamic equations, there are mainly two kinds of differential-algebraic equation solving algorithms and differential equation solving methods [10].

When using ADAMS software for dynamic modeling, the principle is generally from simple to complex, that is to say, the model, that can be used for simulation calculation, is first calculated as a profile model, and then according to the actual needs, the details are added to the profile model to optimize it [11]. The flow of dynamic modeling using ADAMS software is shown in Fig. 2 below.

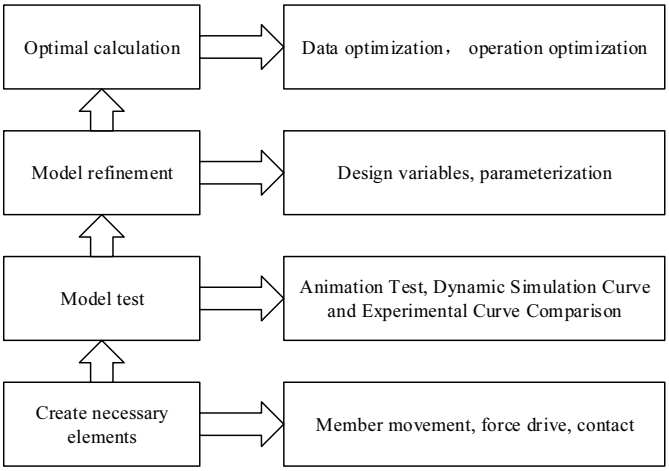

Fig. 2. The flowchart of ADAMS dynamic modeling

3.3.2 Calculation of the Ride Comfort of Armored Vehicles

When the armored vehicle is marching, the wheels are the only ones that make direct contact with the ground, and the external forces suffered by the marching fire of armored vehicle are from the interaction between the tire and the road. Therefore, it is necessary to analyze the impact of armored vehicle tire forces on firing. From the perspective of vehicle dynamics, the analysis and research can be summarized into the research scope of ride comfort. The module of Tire Force in the View environment in the ADAMS software provides a variety of tire models for vehicles under different driving conditions. Therefore, this module is used to model and analyse the tires of armored vehicles. In modeling and analysis, all components are regarded as rigid bodies, and the subsystems are connected by ideal constraints.

In the actual process, armored vehicles will be subject to pitch vibration caused by unevenness of the road surface in the direction of ride and roll vibration caused by different ground effects on the left and right wheels. At present, with the increase of the high and low angles of fire of the armored vehicle system, it is also necessary to consider the influence of the horizontal disturbance of the muzzle caused by the roll vibration of the vehicle. The method of expressing the coherence function of the friction of road surface received by the wheels on both sides is shown below.

$$r(n)=\begin{cases} e^{-pnd} & n\in(n_1,n_2) \\ 0 & n\in(n_1,n_2) \end{cases}. \tag{21}$$

Where: d_v is the wheelbase. ρ is the empirical value, usually it is 1. n_1 and n_2 represent the upper and lower limits of the pavement spatial frequency, respectively.

3.3.3 The Construction of Firing Load model of Wheeled Armored Vehicle

When the wheeled armored vehicle is firing, the calculation method of its launch load p_{pt} is shown below.

$$p_{pt} = \begin{cases} \frac{1}{\psi_p}(1+\frac{1}{2}\frac{\omega}{q})Sp & t < t_g \\ \chi p_g e^{\frac{t-t_g}{b}} & t_g \le t \le t_k \\ 0 & t > t_k \end{cases}. \quad \textbf{(22)}$$

Where: ψ_p represents the secondary work coefficient, and ω is the charge of gunpowder. q is the mass of the projectile, and χ is the characteristic quantity of impulse. P_g is the total force of the barrel at the moment when the projectile exits the muzzle, and b is the time constant of the gunpowder gas. t_g is the instant when the projectile leaves the muzzle, and t_k is the end of the aftereffect period when the projectile leaves the muzzle. S is the cross-sectional area of the barrel, and p is the average pressure of the gunpowder gas.

To calculate the driving force load of marching fire of wheeled armored vehicle, it is necessary to first calculate the driving torque T_t transmitted to the wheels. The calculation method is as follows.

$$T_t = T_{tq} i_g i_0 \eta_T . \quad \textbf{(23)}$$

Where: T_{tq} is the effective torque of the engine, i_o is the main reduction ratio, and η_T is the driveline efficiency of the chassis of the wheeled armored vehicle.

When both the ground and the tire are regarded as rigid bodies, the driving force F_t for each wheel is calculated as follows.

$$F_t = \frac{Tt}{r} = \frac{T_{tq} i_g i_0 \eta_T}{r} . \quad \textbf{(24)}$$

Where: r refers to the rolling radius of the wheel.

The fitting method of driving force is used for calculation and analysis. Thus, it needs to be converted into the sealed traction force F_{ts} acting on the center of vehicle body mass. The conversion method is as follows.

$$F_{ts} = F_{t0} - a_s u_a . \quad \textbf{(25)}$$

Where: F_{t0} represents the initial traction of the vehicle, a_s is the fitting coefficient, and u_a is the speed of the vehicle.

3.4 VR

The rapid development of VR provides people with an artificial environment with multi-sensory functions and realizes human-computer interaction. It has four basic characteristics: multi-sensory, interaction, immersion, and imagination [12].

VR systems are usually composed of input and output devices, model databases, and software platforms. People use computers and input and output devices to realize the interaction between people and VR [13]. The structure of the VR system is shown in Fig. 3 below.

The use of virtual technology to simulate the shooting of armored vehicles during the shooting process aims to be able to use VR to achieve the real situation of marching fire of armored vehicles, so that the relevant personnel can adjust the training process. 3DS MAX is used to establish a virtual technology for model of marching fire of the armored vehicle. The process of building the model is shown in Fig. 4 below.

The modelling tool of 3DS MAX has the features of complete functions and relatively complete animation effects, so the tool is more suitable for establishing a virtual entity model in simulation training system of marching fire of armored vehicle. The model rendered by it is relatively more realistic, which meets the requirements of high simulation of the system and has good portability. Combined with Cry Engine and related virtual reality equipment, the training scene can be simulated realistically. The model flow for building marching fire of armored vehicle is shown in Fig. 5 below.

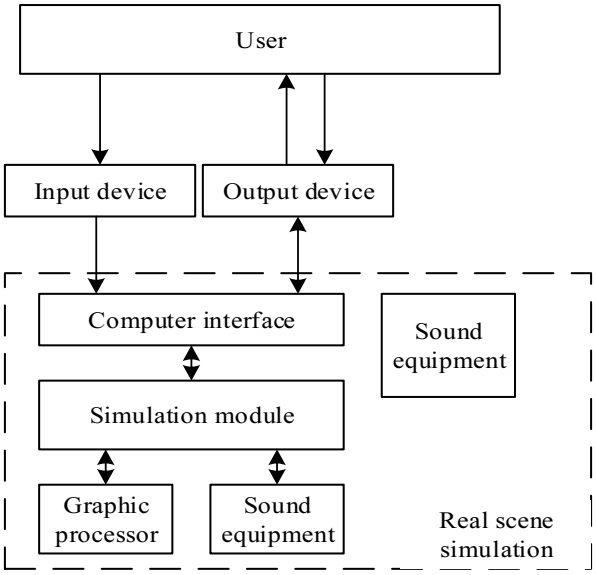

Fig. 3. The structure diagram of the VR system

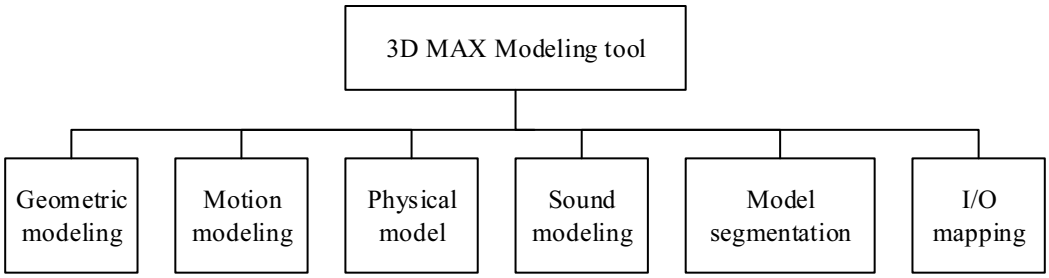

Fig. 4. The flowchart of VR modelling

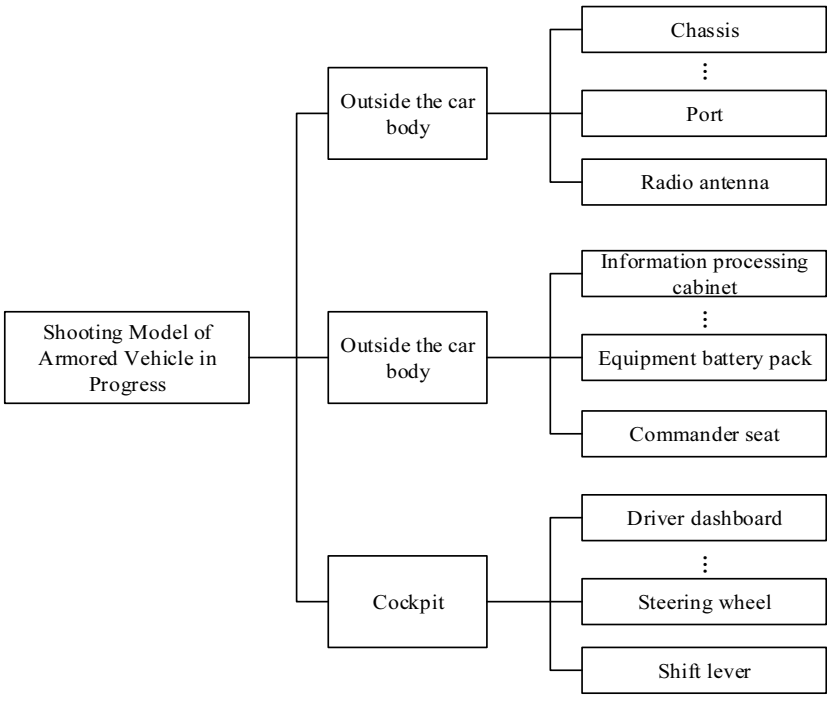

Fig. 5. 3DS MAX model flowchart of marching fire of armored vehicle

4 Result and Analysis

4.1 Verification of the Accuracy of the Dynamic Analysis model of Marching Fire of Armored Vehicle

Before using the dynamic analysis model of marching fire of armored vehicle established above to analyze it, it is needed to verify the accuracy of the model to ensure the accuracy of the analysis results. The calculation results of the vertical displacement of the measuring point at the moment when the projectile comes out of the muzzle and the real test value are used to analyze the error. The number of bursts is 10, of which the high, low, and direction angles of fire are all 0 degrees. The two are kept consistent for analysis. The analysis results are shown in Fig. 6 below.

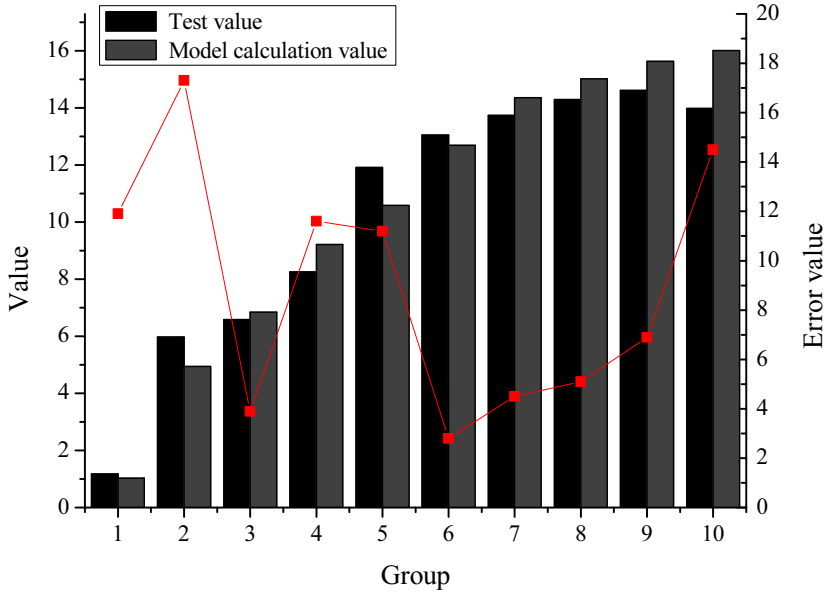

Fig. 6. Error analysis chart of dynamic analysis model of marching fire of armored vehicle

It can be seen from Fig. 6 above that the error range between the dynamic analysis model of armored vehicle shooting and the actual test value proposed is within 15%, indicating that the proposed analysis method has a certain accuracy and can be used to analyse the dynamics of marching fire of armored vehicles.

4.2 Analysis of the Influence of the Actual Driving Condition of Armored Vehicles on the Firing Condition

The dynamic analysis model is used to analyze the firing situation of armored vehicles on different roads. The displacement of high and low angles and direction angles of the firing muzzle under different driving conditions is analyzed. The number of bursts is 10, of which the high and low firing angle is 10 degrees, the directional firing angle is 0 degrees, the trunnion clearance is 0.3mm, and the driving speed is 10km per hour. The roads selected are flat, relatively flat, and uneven roads. The two are kept consistent to analyze the launch state between 3.8 to 4.4s. The analysis results are shown in Fig. 7 below.

Fig. 7 shows that by comparing the displacement curves of high and low angles of the muzzle of the wheeled armored vehicle firing at the same driving speed, it can be seen that when driving on two flat roads, the changes of the displacement of muzzle's high and low angles of the two are consistent. However, when driving on a road with poor flatness, the displacement of muzzle's high and low angles has a large variation value. It can be seen that the poor flatness causes the impact of the chassis system of wheeled armored vehicle to be relatively large, thus causing a more violent reaction. Comparing the displacement curve of direction angle of the muzzle of firing of wheeled armored vehicle at the same driving speed, it can be seen that the firing load is the main factor that causes the displacement of direction angles of the muzzle. When driving on a road with poor road flatness, the change in

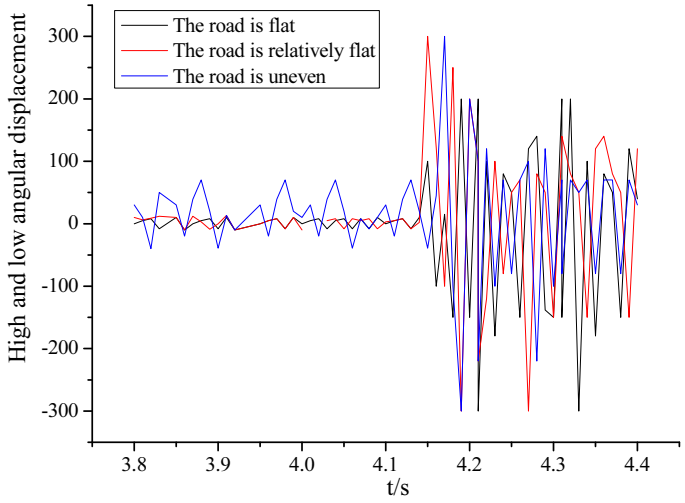

(a) Graph of analysis results of displacement of high and low angles of firing muzzle under different driving conditions

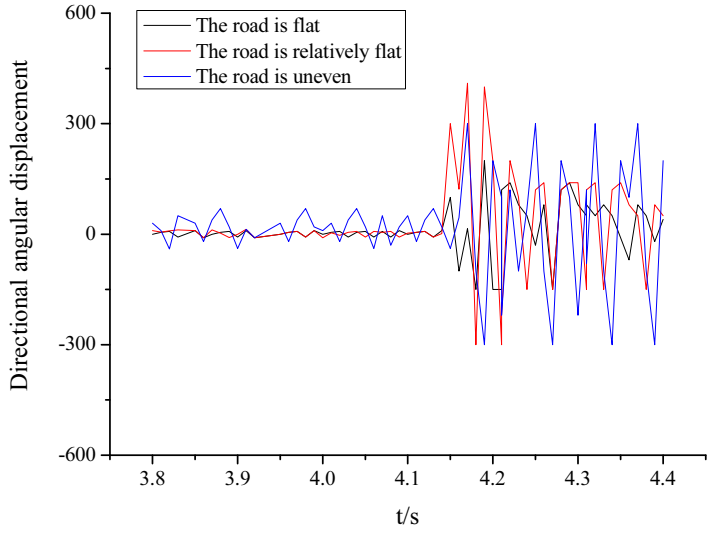

(b) Graph of analysis results of angular displacement of firing muzzle direction under different driving condition

Fig. 7. Analysis results of the displacement of high and low angles and direction angles of the firing muzzle under different driving conditions

displacement of direction angle is relatively small. This is because the effect of road roughness has exceeded the designed load.

4.3 Analysis of the Impact on the High and Low Angles of Marching Fire of Armored Vehicle

The firing targets of wheeled armored vehicles are mainly moving targets in the air. In order to shoot the flying targets in different air layers, the range of the high and low angles of fire of the armored vehicles is also relatively large. The firing dynamics of different high and low angles of fire are analyzed, and the effect of high and low angles of fire on the muzzle is obtained. The values of the high and low firing angles selected in this study are 10 degrees, 40 degrees, and 70 degrees. The directional firing angle is 0 degrees. The number of bursts is also 10 times. It drives on a flat road at a speed of 10km per hour, and the trunnion clearance is maintained at 0.3mm. The analysis results are shown in Fig. 8 below.

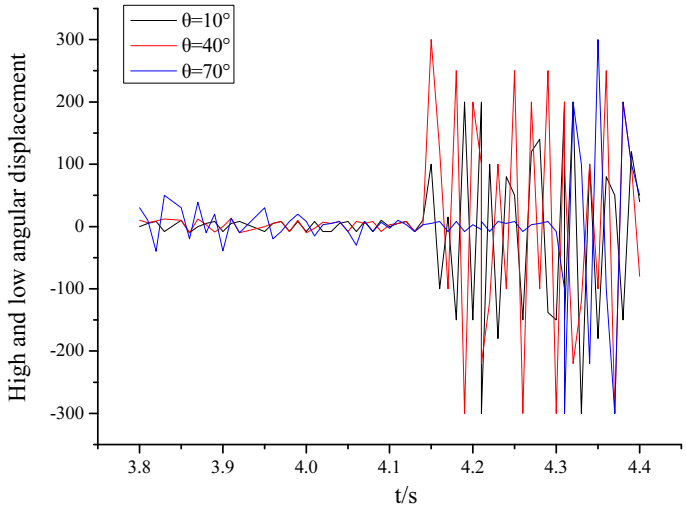

(a) Graph of analysis results of displacement of high and low angles under different high and low angles of fire

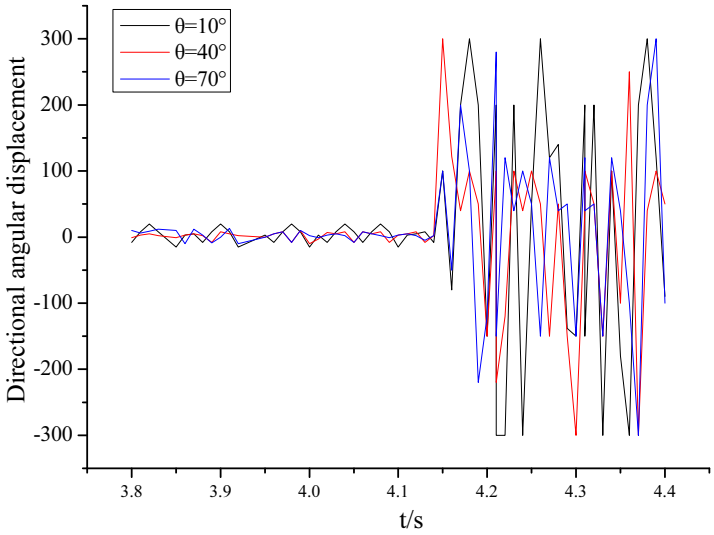

(b) Graph of analysis results of displacement of direction angle under different high and low angles of fire

Fig. 8. Analysis results of displacement of high and low angles and direction angles at different high and low angles of fire

As can be seen from Fig. 8, as the wheeled armored vehicle's high and low angles of fire increase, the displacement of muzzle's high and low angle also increases, and the amplitude of muzzle disturbance also increases. It can be seen that in the range of small firing angle, the gravity torque of the barrel and the inertia torque of the muzzle brake have a certain suppression of the muzzle vibration. When the high and low angles of fire increase, the suppression effect is weakened accordingly, resulting in a large of amplitude of muzzle disturbance. With the increase of the firing angle of the wheeled armored vehicle, the angular displacement of the muzzle direction also increases, and the amplitude of the muzzle disturbance also increases. This is because the angular displacement of the muzzle is mainly affected by the yaw of the vehicle body in the range of small firing angles. Therefore, the range of muzzle disturbance is not large, but due to the increase in the range of high and low angles of fire, the body roll becomes the main influencing factor of displacement of direction angles, resulting in a large range of muzzle disturbance.

4.4 Analysis of the Impact on the Direction of Marching Fire of Armored Vehicle

Based on the dynamic analysis of firing angles in different directions, the effect of directional firing angles on muzzle is obtained. The values of the directional firing angles selected in this study are 0 degrees, 45 degrees, and 90 degrees. The high and low firing angle is 10 degrees. The number of bursts is also 10 times. It drives on a relatively flat road at a speed of 10km per hour, and the trunnion clearance is maintained at 0.3mm. The analysis results are shown in Fig. 9 below.

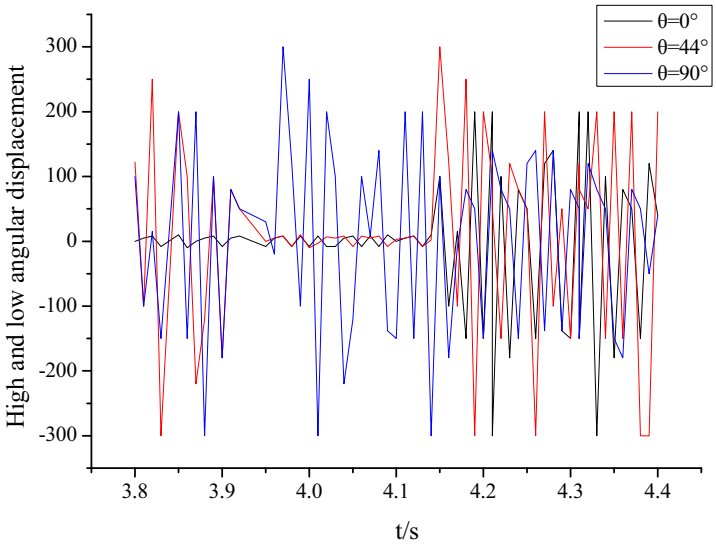

(a) Graph of analysis results of displacement of high and low angles under different directional angles

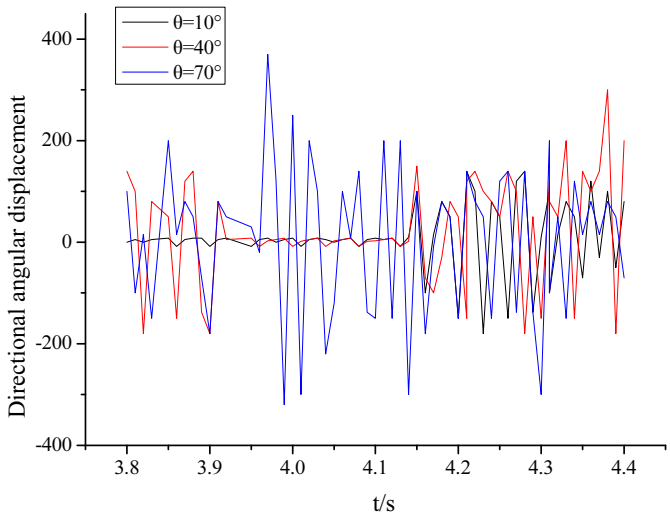

(b) Graph of analysis results of displacement of direction angles at firing angles of different directions

Fig. 9. Analysis results of displacement of high and low angles and direction angles at firing angles of different directions

Fig. 9 shows that as the firing angle of the wheeled armored vehicle increases, the muzzle's displacement of high and low angles increases sharply. It can be seen that the direction of the firing angle changes from small to large, and the disturbance of the shooting load is changed from the pitch moment to the roll moment. The rotary inertia of the vehicle body in the roll direction is much smaller than that in the pitch direction. Under the same load, the deviation of firing direction increases displacement of high and low angles of muzzle. With the increase of the firing angle of the wheeled armored vehicle, the influence of the vibration of the vehicle body on the angular displacement of the muzzle direction also

gradually becomes larger. This is because the increase of directional firing angle makes the main factor that affects the displacement of direction angle of the muzzle change from the roll vibration of the vehicle body to the pitch vibration.

4.5 Analysis of the Effect on the Trunnion Clearance of Marching Fire of Armored Vehicles

The dynamics of shooting between wheeled armored vehicles with different trunnion clearances are analyzed, and the disturbance effect of the trunnion clearances on the firing muzzle is obtained. The trunnion clearance values selected in this study are 0.1mm, 0.3mm, and 0.5mm respectively. The directional firing angle is 0 degrees, the high and low firing angles are 10 degrees, and the number of bursts is also 10 times. It drives on a relatively flat road at a speed of 10km per hour. The analysis results are shown in Fig. 10 below.

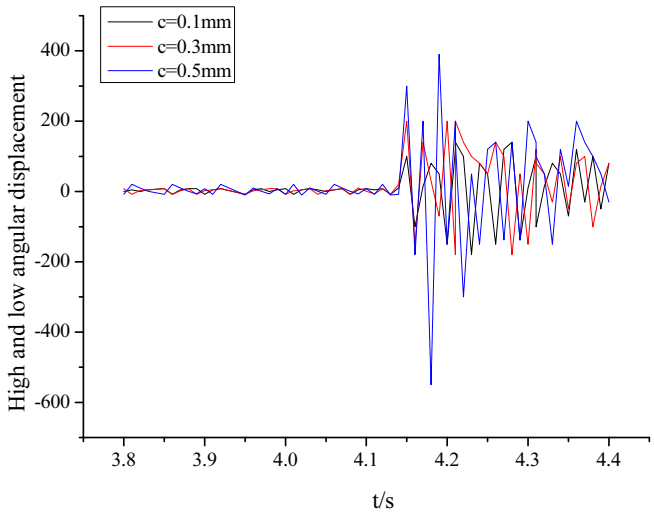

(a) Graph of analysis results of displacement of high and low angles under different trunnion clearances

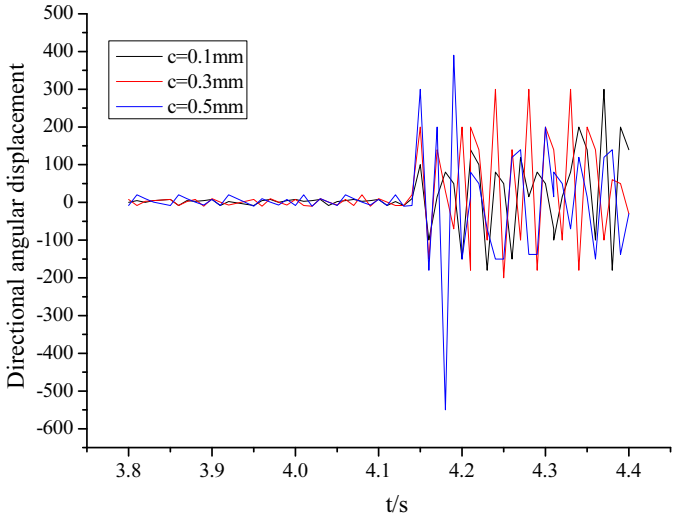

(b) Graph of analysis results of displacement of direction angle under different trunnion clearances

Fig. 10. Analysis results of displacement of high and low angles and direction angles under different trunnion clearances

As can be seen from Fig. 10 above, as the trunnion clearance of the armored vehicle increases, the displacement of its muzzle high and low angles and direction angle increase accordingly. Analysis of the above figure shows that when shooting is not performed, the range of displacement of high and low

angles under several clearances conditions is basically the same. After the shooting starts, as the trunnion clearance increases, the displacement of the muzzle direction angle of the armored vehicle during the shooting also increases. This is because, when shooting, under the condition that the trunnion clearance is larger, the trunnion has a larger movement space in the radial direction. The trunnions on both sides are relatively misaligned, resulting in the displacement of the muzzle's high and low angles and direction angles increases accordingly. Therefore, in the structural design of the armored vehicle, the trunnion clearance of small parameter is more conducive to the armored vehicle to maintain the stability of marching fire.

4.6 Performance Analysis of Dynamic Analysis Model Based on ADAMS Launch Dynamics and VR Technology

The three-dimensional road surface is established by ADAMS dynamics software, and the driving situation on roads with different flatness levels is modeled and analyzed. VR technology is used to simulate reality. Compared with the previous dynamic analysis system, VR technology is added, which allows the operator to truly feel the dynamic characteristics of the armored vehicle under different launch conditions. In this software, different combat environments, combat conditions, and combat equipment can be added and modified. At the same time, the use of this technology facilitates the operation of relevant personnel. It can complete the training of armored vehicle firing without the choice of time and space. There is a clearer and more intuitive understanding of the dynamic characteristics of armored vehicles under different conditions, improving the combat efficiency of relevant personnel.

5 Conclusion

The impact of the dynamic characteristics of marching fire of armored vehicle is mainly studied. Firstly, the analysis of the armored vehicle system is carried out on the assumption of a rigid body, and the analysis system is reasonably simplified to a certain extent. At the same time, the armored vehicle system is reasonably divided and the dynamic equations are established. Secondly, according to the dynamic characteristics of marching fire of armored vehicle, the ADAMS dynamics software is used to construct the dynamic model of marching fire of wheeled armored vehicle, and the VR is used to simulate the marching fire of armored vehicle. Through research, it is found that the deviation range of the dynamic analysis model is within 15%, with a certain accuracy. When driving on a relatively flat road, the changes in displacement of muzzle's high and low angles of the two are consistent. However, when driving on a road with poor flatness, the displacement of muzzle's high and low angular have a large variation value. With the increase of the high and low firing angles, the displacement of muzzle's high and low angles and direction angles also increases, and the amplitude of muzzle disturbance also increases; The increase of the directional firing angle causes the displacement of muzzle high and low angles and direction angles to gradually increase; As the trunnion clearance of the armored vehicle increases, the displacement of high and low angles of its muzzle and direction angles also increases.

Due to the limitation of time and space, in the process of analyzing the dynamic characteristics of marching fire of armored vehicles, only the dynamic characteristics of marching fire of armored vehicles under ideal conditions are considered, but in the actual combat process, the actual situation is much more complicated. Therefore, it is hoped that in the subsequent research and analysis, the analysis can be based on the actual combat environment to make it more comprehensive and reliable.

References

[1] Z. Zhao, C. Liu, B. Chen, B. Brogliato, Asymptotic analysis of Painlevé's paradox, Multibody System Dynamics 35(3)(2015) 299-319.

[2] Z.J. Chen, D.M. Song, H.Y. Xu, Influence of Temperature on Deformation of Barrel During Continuous Firing of a Certain Tank Gun, Zhongbei Daxue Xuebao (Ziran Kexue Ban)/Journal of North University of China (Natural Science Edition) 39(6)(2018) 665-671.

[3] Q.C. Zha, X.T. Rui, H.L. Yu, Q.B. Zhou, Study on the impact sensitivity of firing factors of self-propelled gun, Zhendong Gongcheng Xuebao/Journal of Vibration Engineering 30(6)(2017) 938-946.

[4] J. Balla, Z. Krist, C.I. Le, Experimental study of turret-mounted automatic weapon vibrations, International Journal of Mechanics 9(1)(2015) 16-25.

[5] H. Xie, H.Y. Wang, Q. Rui, S.L. Li, Y. Duan, Finite Element Modeling and Modal Matching Analysis of Tracked Vehicle Turret and Gun, Journal of Academy of Armored Force Engineering 32(4)(2018) 63-68.

[6] Z.A. Kadir, K. Hudha, H. Zamzuri, S.A. Mazlan, M. Murrad, F. Imaduddin, Modeling, validation and firing-on-the-move control of armored vehicles using active front-wheel steering, Journal of Defense Modeling & Simulation Applications Methodology Technology 13(2)(2016) 253-267.

[7] Q.L. Song, Z.G. Lu, W. Wang, Z.M. Fan, X.Y. Zhai, Prediction Model Research of Vibration Angle Errors of Armored Vehicle Muzzle on Move, Fire Control & Command Control 44(4)(2019) 121-125.

[8] V.R. Aparow, K. Hudha, Z.A. Kadir, M. Mansor, N.H. Amer, 2016 SICE International Symposium on Control Systems (ISCS), 2016.

[9] C.Y. Chang, G. Han, Simulation Research of Chain Transmission Mechanism Based on MSC__ADAMS Platform, Journal of Taiyuan University of Science and Technology 42(4)(2018) 287-292.

[10] C. Li, L. Xian, Y. Liu, Y. Liao, Simulation Analysis on Double Row Tapered Roller Bearings with Typical Faults in High-Speed Locomotive Based on ADAMS, Bearing (6)(2018) 55-59.

[11] Y.L. Han, H.H. Guo, H. Zheng, Research on Coordinated Simulation of Lifting Mechanism of Garbage Truck Using ADAMS and MATLAB, Machinery Design & Manufacture 56(7)(2018) 184-187.

[12] R. Skibba, Virtual reality comes of age, Nature 553(7689)(2018) 402-403.

[13] M.S. Elbamby, C. Perfecto, M. Bennis, K. Doppler, Toward Low-Latency and Ultra-Reliable Virtual Reality, IEEE Network 32(2)(2018) 78-84.